Temperature compensation model of MEMS inertial sensors based on neural network

Golrokh Araghi, René Jr Landry
Department of electrical engineering
École de technologie supérieure
Montreal, Canada
Golrokh.araghi@lassena.etsmtl.ca, ReneJr.Landry@etsmtl.ca

***Abstract*—Micro-electromechanical Systems (MEMS) inertial sensors are lightweight, small size and low-cost sensors that consume less power energy compared to their high-precision bulky counterparts. However, this miniaturization is a double-edged sword and MEMS-based inertial sensors suffer from various error sources, noises and instabilities. Indeed, inertial sensor errors vary with time, temperature and from turn on to turn on. In order to exploit the full potential of a MEMS-based inertial navigation system (INS), and to enhance its accuracy, it is indispensable to develop a temperature-dependent model that compensates these errors. Traditional temperature compensation methods rely on polynomial regression method, which fails to take into account the nonlinearities inherent in the sensor errors. This paper proposes a new temperature compensation model for a full inertial measurement unit (IMU), based on a radial basis function neural network (RBFNN) that compensates the significant deterministic errors of both accelerometer and gyroscope triads in a wide temperature range. A high precision rate table and a thermal chamber are used for accurate testing. The effectiveness of the method is investigated with various static and dynamics tests in the laboratory and with a car, and results are compared with the traditional polynomial fitting method.**

Keywords— inertial sensor; thermal calibration; neural network; MEMS IMU; navigation.

I. INTRODUCTION

With the advent of the Micro-electromechanical Systems (MEMS) technology, it is now possible to produce miniature inertial sensors that are fabricated with their electronic circuits and other mechanical components on a common substrate [1]. MEMS-based inertial sensors have the advantage of small size, light weight, low cost, low power consumption and high reliability [2]. However, relative to macro-scale inertial sensors, MEMS inertial sensors are more prone to error sources and noise. Moreover, the effect of environmental conditions especially temperature variations on the MEMS inertial sensors outputs is more prominent relative to their conventional counterparts. In fact, the main substance of MEMs inertial sensors is silicon, whose physical characteristics vary with the temperature. Sensor's packaging and electronics are also highly sensitive to temperature variations. Inertial sensor designers often make the following comment: "No matter what sort of sensor we design, it always turns out to be a highly sensitive thermometer!" [3].

Because of the integration process performed in the inertial navigation, the uncompensated errors will grow without bound over time and make the navigation completely inaccurate in a short period of time. For example, an uncompensated bias of 5 °/s in gyroscope measurements will introduce a position error of 142 m in only 10 s [4].

Normally, inertial navigation systems (INS) and global navigation satellite systems (GNSS) are integrated into a hybrid system, in which the GNSS signal is responsible for regular correction for the INS, while the INS is used to provide navigation information in challenging environments, where GNSS signals are unavailable or unreliable. Therefore, it is essential to develop a temperature-dependent model for MEMS inertial sensors, to enhance the overall system accuracy such that it can work properly in stand-alone mode in GNSS-denied environments for land vehicle navigation applications.

There are mainly two methods for eliminating the errors caused by the temperature, and both have been extensively investigated in the literature. The first is a temperature control method based on a machining technique and using an experimental approach [5], [6], [7], [8]. This method results in a great stability and high accuracy, but the accuracy comes at a high price, and requires a complex design and maintenance.

The second method is called the temperature compensation, also known as the phenomenological method. It eliminates temperature-induced errors by filtering and mathematical modeling using software technology. Although the first method is much more precise, the complexity and the cost of mathematical modeling is significantly less than temperature control technologies. This is why the temperature compensation based on mathematical modeling is employed in this paper.

Traditionally, polynomial regression techniques have been used for developing a temperature-dependent model for inertial sensors errors. References [9] and [10] both used a third-order polynomial to compensate temperature errors. In [11], a simple linear interpolation was proposed. For thermal calibration of a fiber optic gyroscope (FOG), [12] used a stepwise linear regression method to establish the relationship between the input rotation rate, the output voltage and the internal temperature of the sensor.

The concept of employing a neural network to serve as a temperature compensation model is not new. In [13], a radial

978-1-5386-1647-5/18/$31.00 ©2018 IEEE

basis function neural network (RBFNN) was used to compensate the temperature drift of a FOG. To reduce the randomness inherent in the data, [14] used a gray radial basis function neural network to reduce the temperature dependency of the FOG output.

The use of backpropagation (BP) neural networks to compensate the bias drift of the gyroscope has also been widely employed in the literature [15],[16],[17]. The temperature dependency of a MEMS torsional accelerometer was modeled in [18], through a Levenberg-Marquardt backpropagation (LM-BP) neural network, which has the advantage of faster convergence and more precise fitting relative to a regular BP neural network.

Other neural network-based strategies have also been proposed by a number of authors, such as the Elman neural network [19] or a simple feedforward neural network, where the learning rate of the neural network is adapted by fuzzy logic rules [20]. For compensating the bias drift of a MEMS gyroscope, an adaptive compensation algorithm based on a strong tracking Kalman filter (STKF) was proposed in [21], which makes use of the support of compass orientation measurements. The parameters of the model are not fixed; rather they intelligently adapt themselves in a changing environment. Because of integration with a compass, the algorithm does not work well in locations where there are magnetic interferences. The advantage is that the compensation method is online, which eliminates the need to calibrate the temperature errors before use.

To model the dynamic angular velocity of a FOG and compensate temperature-dependent errors, [22] proposed a compensation method based on a RBFNN, providing a nonlinear mapping between the true value of angular velocity, the gyroscope output voltage and the temperature. Later, to improve the sensitivity of the model, the same author proposed to find the nonlinear relationship between the angular velocity error (which is considered as the difference between angular velocity and its nominal value), the gyroscope output voltage and the temperature instead of considering the true angular velocity value [23].

In this paper, temperature compensation of inertial sensors is considered as a function approximation problem, and the inertial sensor errors are modeled as a function of the temperature and of the sensor output measurements. The difference with previous studies is that with the proposed method, both accelerometer and gyroscope triads can be compensated. Moreover, in order to evaluate the performance of the method, various static and dynamic tests in temperature changing situations have been performed, which has been barely addressed in the similar works.

The remainder of this paper is organized as follows: the measurement model of the inertial sensors is presented in Section II. The calibration procedure for finding the coefficient of the measurement model is explained in Section III. The polynomial regression and the neural network-based thermal compensation methods are discussed in detail in Section IV. Test set-up, data acquisition and experimental results are provided in Section V, and finally, the conclusion and future works are given in Section VI.

II. Sensor error model

The first step for calibrating the inertial sensors is to define a measurement model that relates the output signal of the sensors to their inputs through a mathematical expression. The unified sensor error model is defined as [24]:

$$\tilde{\mathbf{u}}_k = \mathbf{S}_k\mathbf{u}_k + \mathbf{b}_k + \mathbf{w}_k$$
$$\begin{bmatrix}\tilde{u}_x\\ \tilde{u}_y\\ \tilde{u}_z\end{bmatrix}_k = \begin{bmatrix}s_{xx} & m_{xy} & m_{xz}\\ m_{yx} & s_{yy} & m_{yz}\\ m_{zx} & m_{zy} & s_{zz}\end{bmatrix}_k \begin{bmatrix}u_x\\ u_y\\ u_z\end{bmatrix}_k + \begin{bmatrix}b_x\\ b_y\\ b_z\end{bmatrix}_k + \begin{bmatrix}w_x\\ w_y\\ w_z\end{bmatrix}_k . \quad (1)$$

The index k represents the type of sensor (a for accelerometer and g for gyroscope) and applies to all the elements of the matrix or vector. The vector $\tilde{\mathbf{u}}_k$ is the measured physical quantity by the sensor (specific force for the accelerometer and angular velocity for the gyroscope), the vector $\mathbf{u}_k$ is the expected value of the sensors (true value), the matrix $\mathbf{S}_k$ is a unitless matrix that includes the scale factor errors (diagonal elements) and the misalignment errors (non-diagonal elements). The vector $\mathbf{b}_k$ is the bias and the vector $\mathbf{w}_k$ is zero mean white noise. The units for vectors $\tilde{\mathbf{u}}_k$, $\mathbf{u}_k$, $\mathbf{b}_k$, and $\mathbf{w}_k$are g for the accelerometer (1 g = 9.80665 m/s²) and °/s for the gyroscope.

In the next section, the procedure to find the coefficients of this error model is explained.

III. Calibration procedure

Calibration is defined as the process of determining the coefficients of the sensor measurement model [3]. The most commonly used calibration technique in the literature is the six-position calibration method [25],[4]. In this method, the IMU is oriented with each sensitive axis alternatively up and down relative to the local gravity; this results in six different orientations. For an accelerometer triad, the error terms are determined by comparing the magnitude of the measured specific force in three axes with the magnitude of the local gravity vector. Since the Earth's rotation rate is very low (15 °/h), it cannot be measured by low-cost MEMS gyroscopes. Therefore, a single axis rate table is used as a reference value for the gyroscope calibration. After recording the sensors output, at each orientation, measurements are averaged; note that after averaging the noise terms will be negligible since they are assumed to be zero mean white noise. Taking into account measurements from six orientations, Eq (1) takes the following form:

$$\tilde{\mathbf{U}}_k = \mathbf{E}_k\mathbf{U}_k, \quad (2)$$

where:

$$\tilde{\mathbf{U}}_k = \begin{bmatrix}\tilde{u}_x^{Xup} & \tilde{u}_x^{Xdn} & \tilde{u}_x^{Yup} & \tilde{u}_x^{Ydn} & \tilde{u}_x^{Zup} & \tilde{u}_x^{Zdn}\\ \tilde{u}_y^{Xup} & \tilde{u}_y^{Xdn} & \tilde{u}_y^{Yup} & \tilde{u}_y^{Ydn} & \tilde{u}_y^{Zup} & \tilde{u}_y^{Zdn}\\ \tilde{u}_z^{Xup} & \tilde{u}_z^{Xdn} & \tilde{u}_z^{Yup} & \tilde{u}_z^{Ydn} & \tilde{u}_z^{Zup} & \tilde{u}_z^{Zdn}\end{bmatrix}_k ,$$

$$\mathbf{E}_k = \begin{bmatrix}s_{xx} & m_{xy} & m_{xz} & b_x\\ m_{yx} & s_{yy} & m_{yz} & b_y\\ m_{zx} & m_{zy} & s_{zz} & b_z\end{bmatrix}_k ,$$

$$\mathbf{U}_{\mathrm{k}} = \begin{bmatrix} K & -K & 0 & 0 & 0 & 0 \\ 0 & 0 & K & -K & 0 & 0 \\ 0 & 0 & 0 & 0 & K & -K \\ 1 & 1 & 1 & 1 & 1 & 1 \end{bmatrix}_{\mathrm{k}}.$$

The matrix $\widetilde{\mathbf{U}}_{\mathrm{k}}$ is the measurement matrix in which each column corresponds to one orientation of the IMU. The upper index Xup means that the x-axis is in the up direction, and Xdn means that the x-axis is in the down direction; thus for example $\tilde{u}_{\mathrm{y}}^{\mathrm{Xup}}$ is the value measured by the sensor along the y-axis when the x-axis is in the up direction. The matrix $\mathbf{E}_{\mathrm{k}}$, is the error matrix containing all the error terms. Finally, the matrix $\mathbf{U}_{\mathrm{k}}$ is the reference matrix in which K is a known reference value (local gravity for the accelerometers and known angular velocity from the rate table for the gyroscopes). The estimated error matrix can then be determined by the ordinary least square method as:

$$\hat{\mathbf{E}}_{\mathrm{k}} = \widetilde{\mathbf{U}}_{\mathrm{k}}\mathbf{U}_{\mathrm{k}}(\mathbf{U}_{\mathrm{k}}\mathbf{U}_{\mathrm{k}}{}^{\mathrm{T}})^{-1}. \quad (3)$$

This is the basic method for obtaining inertial sensors systematic errors including bias, scale factor and misalignment. The next section explains the procedure for modeling the sensors behavior at different temperature points.

IV. Thermal Calibration

A. Thermal tests

Two thermal tests were introduced by Titterton in [25], the soak test and the ramp test. In the first method, the IMU is mounted inside a thermal chamber and after stabilization time, which is considerably long, the measurements are recorded. In the ramp method, on the other hand, the temperature of the thermal chamber is decreased or increased linearly, and the whole test takes just a few minutes to complete. In [9], the soak method was employed and a temperature model based on a third-order polynomial fitting was developed. Reference [11] has implemented both the ramp and the soak methods and has demonstrated that the results from the ramp method are not as accurate as the soak method, since the sensors require considerably long period of time to stabilize. The thermal test implemented in this work is therefore based on the soak method.

The IMU is mounted on a rate table that is enclosed inside a thermal chamber. For each temperature point, the calibration procedure is repeated. At the end of the process, a series of error terms along with their corresponding temperatures are obtained. Any correlation between these errors and temperature variations can then be defined through a mathematical expression or a look-up table.

B. Polynomial regression method

Traditionally, polynomial regression methods are used to model the inertial sensors based on the temperature. In statistics, regression includes all the techniques for modeling and analyzing the trend between some dependent and independent variables. One class of linear regression is the polynomial regression, where the relationship between the input and the output variable is described as an n^{th}-order polynomial. The polynomial model of the n^{th} degree with one variable is given by:

$$p(x) = p_n x^n + p_{n-1}x^{n-1} + \cdots + p_1 x + p_0, \quad (4)$$

where $\{p_i\}_{i=0}^{n}$ are the polynomial coefficients and x is the independent variable. In the application of thermal calibration of inertial sensor errors, the independent variable is considered to be the temperature, denoted T, and the dependent variable is the error term (bias, scale factor or misalignment).

This is important to find the optimum order of the polynomial to fit the data. As the order of polynomial increases, the sum of squares of the residuals decreases, however, a higher order for the polynomial is not always a better choice since at some point, it may over-fit the data. Not to mention that the computation load will also increase. The order of the polynomial depends on the type of data and should be determined statistically such that the best fit to the data with the minimum sum of squared residuals is obtained. In this work, a third order polynomial is used for modeling the scale factor, bias and misalignment, respectively:

$$\begin{aligned} b(T) &= b_3T^3 + b_2T^2 + b_1T + b_0, \\ S(T) &= s_3T^3 + s_2T^2 + s_1T + s_0, \\ m(T) &= m_3T^3 + m_2T^2 + m_1T + m_0. \end{aligned} \quad (5)$$

The parameters b_i, s_i and m_i, $i = 0,1,2,3$ are then stored in a microcontroller and can be used for online compensation of the inertial sensors.

C. Radial basis function neural network

Temperature compensation of inertial sensors can be regarded as a function approximation problem. A common challenge in the statistic is approximating a function from some input-output example pairs without any *a priori* information about the function. In the neural network concept, function approximation problem is the task of the supervised learning. and these input-output pairs are called training set [26]:

$$\mathcal{T} = \{(\mathbf{x}, y)\}_{i=1}^{p}, \quad (6)$$

where, p is the number of available pairs, $\mathbf{x}$ is the input vector $(n \times p)$ with n being the number of features (elements of the input) and y being the output $(p \times 1)$. The desired unknown function h is learned from the training example:

$$y = h(\mathbf{x}). \quad (7)$$

The neural network is provided with a set of labeled training examples, which means that for each input, there is an associated output. The first step is the training phase, where the difference between the desired output of the network and its actual output is used to adjust the parameters of the network. This adjustment is repeated until certain statistical criteria are satisfied. At this point, the parameters of the network will be stored and used for the prediction phase, where a set of unlabeled inputs are given to the network and it can estimate the corresponding output completely by itself [27].

There are different neural topologies that can be utilized as function approximation tool. The RBF and MLP (multilayer perceptron) are the most commonly used neural networks for this application. Compared to MLP, RBF has a faster training process and performs more robustly when fed with noisy inputs. Another MLP's drawback is that, in the search for global minima in the complex search space, the MLP is likely to get trapped in an undesirable local minima [28]. This is why radial RBFNN has been employed in this study.

The radial basis function neural network has a feedforward architecture consisting of three layers. The first layer is the input layer, which does not do any processing. The second layer is called the hidden layer, and is responsible for performing a nonlinear mapping from the input space to the output space. The activation function at the hidden layer is a radial basis function whose response decreases or increases monotonically with distance from a central point. Normally, the radial basis function is chosen to be Gaussian:

$$\varphi(x) = \exp\left(\frac{-\|x-c\|^2}{2r^2}\right), \tag{8}$$

where $\|\cdot\|$ is the Euclidian distance, $\mathbf{c}$ and r, are the parameters of the radial basis function representing the center and the width (radius) of the Gaussian RBF, respectively.
Finally, the output layer is simply a linear combination of the outputs of the neurons in the hidden layer:

$$h(\mathbf{x}) = \sum_{j=1}^{m} w_j \varphi_j(\mathbf{x}), \tag{9}$$

where w_j are the weights between the hidden and output layers and m is the number of hidden units. The idea behind the RBFNN is to interpolate the target function to be approximated, by using a linear superposition of a number of radial basis functions. The training of RBFNN is done in two steps. First, the center and width of hidden neurons are chosen, and in the second step, the weights of the hidden neurons are determined through minimizing the following cost function:

$$J(w) = \sum_{i=1}^{p}\left(y_i - h(\mathbf{x}_i)\right)^2 + \sum_{j=1}^{m} \lambda_j w_j^2, \tag{10}$$

where the additional term λ is the regularization factor that penalizes the overall complexity of the model such that models with a higher value of weights cost more. It is used for improving the neural network performance and to prevent overfitting.

D. Applicatipon of radial basis function neural network for temperature drift modeling of inertial sensors

The nonlinear mapping between the sensors measured value ($\tilde{u}$), the temperature (T) and the error (Δu) can also be obtained by employing a radial basis function neural network (RBFNN) to be used as a tool for function approximation. The schematic of this network is illustrated in Fig. 1. In this method, the error terms are not modeled separately and they are all lumped together in Δu, which is considered to be the difference between the measured and the true value of the sensor. Since it is desired to investigate the effect of the temperature on the sensor errors, the temperature and the measured value of the sensor are chosen to be the input of the network, and the error signal is selected to be the network output.

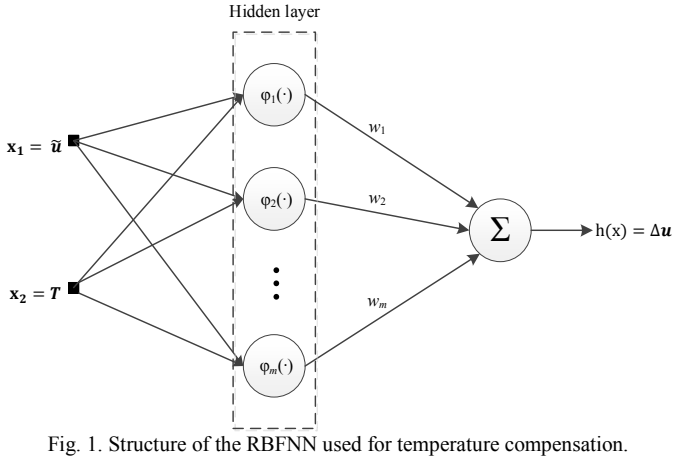

Fig. 1. Structure of the RBFNN used for temperature compensation.

The network is trained by performing forward selection using orthogonal least squares. Forward selection algorithm builds a model that uses only a subset of the available radial basis functions; it starts with an empty subset, and at each iteration one radial basis function is added to the subset, until some criterion is satisfied. The advantage of the forward selection algorithm is that there is no need to fix the number of hidden units in advance. Generalized cross validation is used for model selection criterion. At the end of the process, there are six different neural network for each sensor (three accelerometer and three gyroscopes) with their corresponding parameters.

In the compensation phase, the trained networks are provided with the measured value of the sensors along with their corresponding temperatures, and the networks estimate the associated error. Adding this estimated error to the measured value by the sensor will then yield the compensated values by the network:

$$\hat{u} = \widehat{\Delta u} + \tilde{u}, \tag{11}$$

where $\hat{u}$ is the compensated value by the network and $\widehat{\Delta u}$ is the sensor error estimated by the neural network.

V. Results and Discussion

A. Test set-up and data acquisition

The inertial measurement unit used in this study is a custom-made IMU developed in the laboratory of LASSENA consisting of three MEMS accelerometers and three MEMS gyroscopes from STMicroelectronics. The specification of the sensors can be found in TABLE 1. A high precision single axis rate table with the velocity accuracy of ±0.01 % enclosed in a thermal chamber is used to provide reference measurements for the gyroscope tirade (Fig. 2). The IMU is mounted on the rate table, and the thermal chamber temperature is changed between –25 °C and 55 °C with a step of 5 °C. On the other hand, at each temperature point, the angular velocity is also changing automatically in a triangular pattern with the minimum velocity of –100 °/s and the maximum velocity of 100 °/s with a step of 10 °/s. After allowing the sensors to stabilize at the given

TABLE 1. INERTIAL SENSORS SPECIFICATIONS.

Sensor	Accelerometer	Gyroscope
Model	LSM303DLHC	L3GD20
Noise density	220 μg/$\sqrt{\text{Hz}}$	0.03 (°/s)/$\sqrt{\text{Hz}}$
Sensitivity	1 mg/LSB	8.75 m(°/s)/digit
Bias range	±60 mg	±10 °/s
Sensitivity change vs. temperature	± 0.01 %/°C	± 2%
Bias change vs. temperature	±0.5 mg/°C	± 0.03 °/s/°C

Fig. 2. Single axis rate table enclosed in the thermal chamber.

temperature, the angular velocity measurements are recorded during 60 s at the sampling frequency of 50 Hz. At the end of the test, about 3 million samples are recorded per each orientation for the 17 temperature steps and 40 angular velocity steps, and the whole test takes almost 4 days to be completed.

B. Experimental results

First, based on the six-position calibration method explained previously, at each temperature step, the bias, scale factor and misalignment are calculated for each axis. Then these systematic errors and their corresponding temperatures are modeled with a third order polynomial. Fig. 3 to Fig. 6 show the modeled polynomial function fitted to the bias and the scale factor at different temperatures. It can be seen that the bias and the scale factor change significantly with the temperature variation, and although the sensors in different axes of the IMU are from the same manufacturer, they do not exhibit the same behaviour over temperature. For example, accelerometer bias along z-axis can vary between −80 mg and 110 mg in the whole temperature range, which is huge; in average, it changes of −2.32 mg per degree Celsius which is higher than the ±0.5 mg/°C stated by the datasheet of the sensors. This bias if

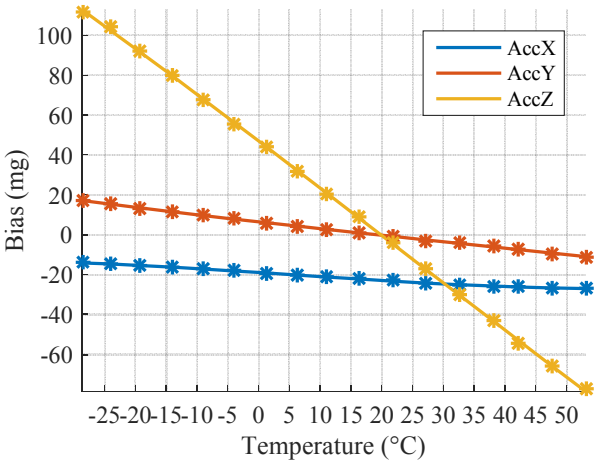

Fig. 3. Third-order polynomial function fitted to the accelerometer bias at different temperatures.

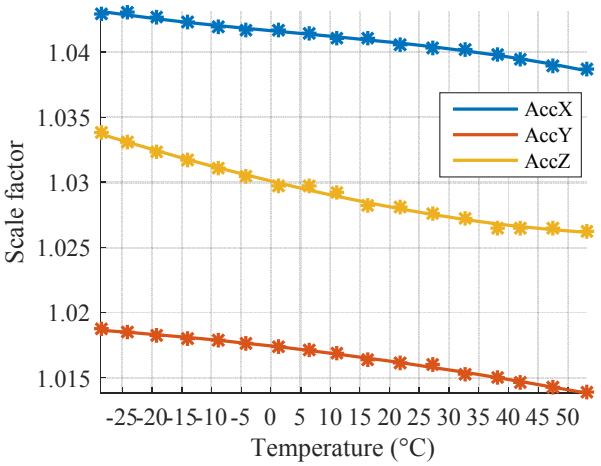

Fig. 4. Third-order polynomial function fitted to the accelerometer scale factor at different temperatures.

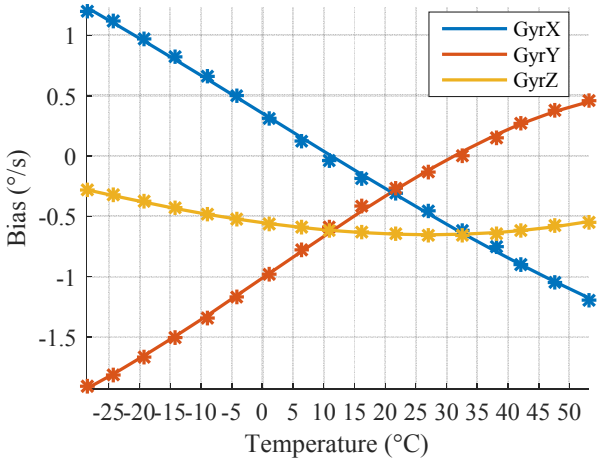

Fig. 5. Third-order polynomial function fitted to the gyroscope bias at different temperatures.

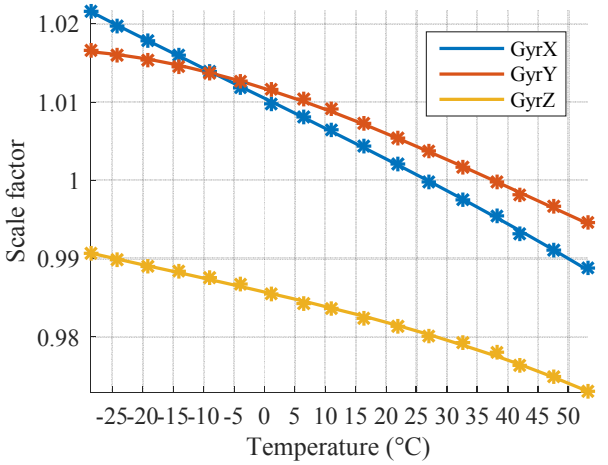

Fig. 6. Third-order polynomial function fitted to the gyroscope scale factor at different temperatures.

not compensated will lead to a huge error in the navigation solution.

In the second step, the neural network is trained with the training dataset, which consists of 80 % of the whole sensor output measurements from six different orientations selected randomly, and the remaining 20 % of the measurements are used as the validation set. After training, the parameters of the trained network, (including the weights, centers and radius of the hidden layer) are then stored and applied to the validation dataset to verify its performance.

As an example, Fig. 7 and Fig. 8 show the error (the difference between the reference and estimated value by the network) before and after applying the compensation algorithm on the validation set for the accelerometer and the gyroscope along the x-axis, respectively. For the accelerometer the average error has decreased from 21.55 mg to about 5×10^{-4} mg, and for the gyroscope this value has decreased from 0.1414 °/s to about 2×10^{-5} °/s after compensation. In both cases, there has been more than 99 % improvement on the mean and the standard deviation of the error after applying neural network compensation.

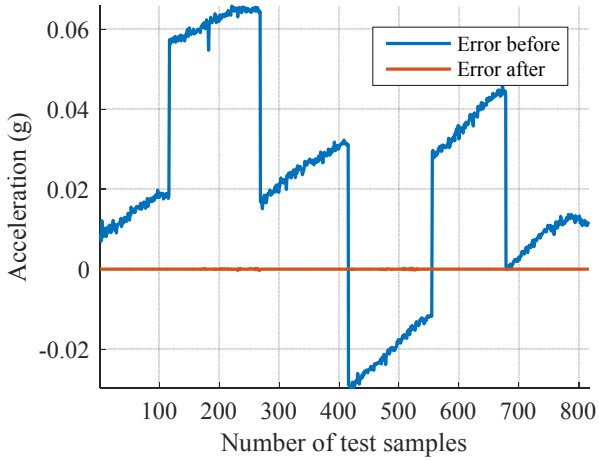

Fig. 7. Error before and after neural network compensation on the validation dataset for the accelerometer along the x-axis.

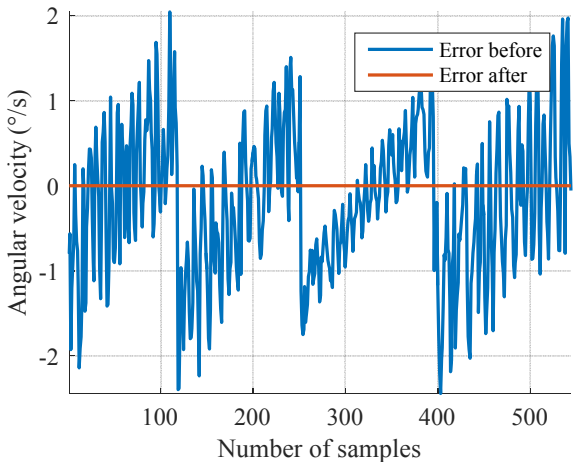

Fig. 8. Error before and after neural network compensation on the validation dataset for the gyroscope along the x-axis.

C. *Verification of results with real tests*

In order to compare the performance of the polynomial regression and neural network compensation model, several tests have been performed. These tests include: 1. A static test in the laboratory, where the temperature of the IMU is changed. 2. Moving the IMU manually in a predefined straight line in the laboratory. 3. A dynamic test outside with a car.

For the first test, in the laboratory, the IMU is placed on a leveled surface and kept stationary while being heated with a heater gun. The internal temperature of the IMU has changed from 22 °C to 51 °C (Fig. 9). The static output measurements from the IMU are then recorded for the duration of 20 minutes at the sampling frequency of 200 Hz. The norm of the measured acceleration and angular velocity, obtained from the measurements of three axes, with and without compensations are illustrated in Fig. 10 and Fig. 11, respectively. The average of acceleration norm is 1.0555 g, before compensation, 1.03332 g after polynomial compensation, and 1.0009 g after neural network compensation, where the expected acceleration norm is 1 g since the IMU is stationary. Thus, with the polynomial fitting method there is a 40 % improvement whereas with the neural network approach, there is a 98 % improvement on the average norm of measured acceleration. Regarding the gyroscope, the average norm of measured angular velocity is 1.1032 °/s before compensation, 0.6805 °/s after polynomial compensation and 0.0010 °/s after neural network compensation. Thus, with the polynomial method, there is only 38 % improvement whereas with the neural network compensation method, there is a 99 % improvement on the average norm of angular velocity. TABLE 2 and TABLE 3 list the mean and the standard deviation of the error of the 20-minute static measurements before compensation and after applying each compensation model for each individual sensor.

The polynomial regression method can decrease the accelerometer error up to 69 %, for the gyroscopes along x- and

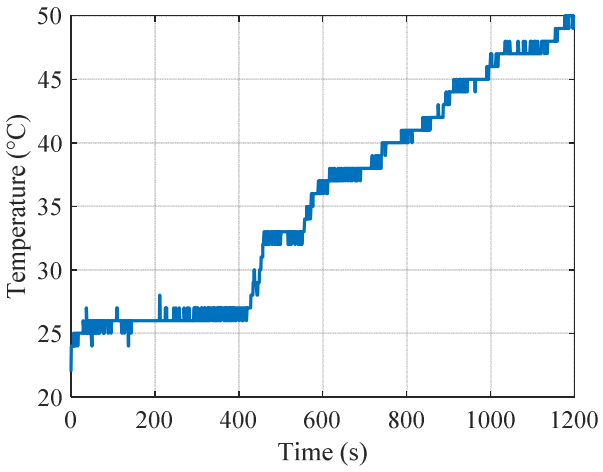

Fig. 9. Internal temperature of the gyroscope of the static IMU for 20 minutes while being heated with a heater gun.

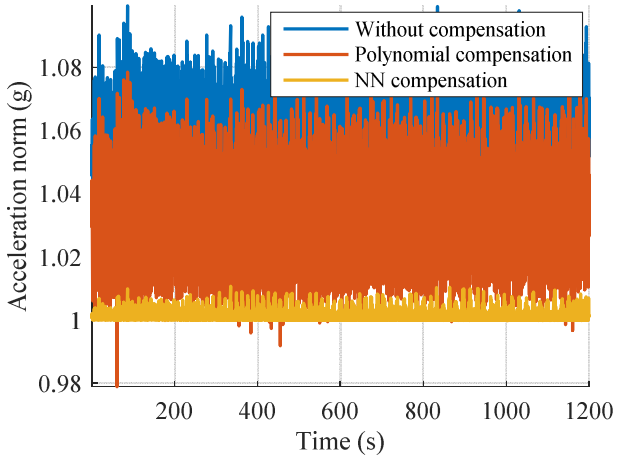

Fig. 10. Norm of the acceleration before and after compensation of the static IMU while being heated with a heater gun.

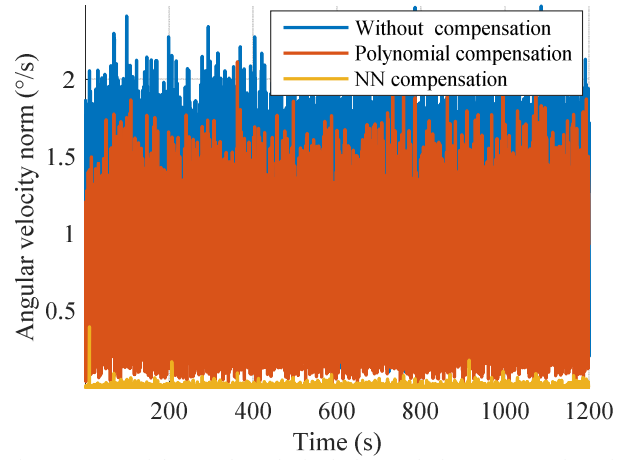

Fig. 11. Norm of the angular velocity before and after compensation of the static IMU while being heated with a heater gun.

z-axis, there is an improvement of 60 % and 87 % on the average error, respectively; however, it can be seen that there is no improvement along the y-axis. In general, according to the obtained results, it can be observed that with the polynomial fitting method, better performance can be achieved for

TABLE 2. MEAN AND STANDARD DEVIATION OF ACCELEROMETERS ERRORS (g) BEFORE AND AFTER COMPENSATION ON 20-MINUTE STATIC DATA WHILE BEING HEATED.

	Accelerometer X		Accelerometer Y		Accelerometer Z	
	Mean	Standard deviation	Mean	Standard deviation	Mean	Standard deviation
Raw data	0.06096	0.45898	0.12214	0.83358	0.50019	0.09843
Polynomial fitting	0.01843	0.44236	0.06756	0.81955	0.28262	0.09194
Improvement (%)	69.76	3.62	44.68	1.68	43.49	6.59
Neural network	0.00059	0.00679	0.02611	0.26529	0.00586	0.00632
Improvement (%)	99.02	98.51	78.62	68.17	98.82	93.57

TABLE 3. MEAN AND STANDARD DEVIATION OF GYROSCOPES ERRORS (°/s) BEFORE AND AFTER COMPENSATION ON 20-MINUTE STATIC DATA WHILE BEING HEATED.

	Gyroscope X		Gyroscope Y		Gyroscope Z	
	Mean	Standard deviation	Mean	Standard deviation	Mean	Standard deviation
Raw data	0.57649	0.35439	0.02682	0.44803	0.74171	0.32338
Polynomial fitting	0.22557	0.35323	0.22268	0.44506	0.09609	0.32961
Improvement (%)	60.87	0.32	-730.2	0.66	87.04	-1.92
Neural network	0.00001	0.00100	0.00079	0.00335	0.00000	0.00380
Improvement (%)	99.99	99.71	97.04	99.25	99.99	99.82

accelerometer rather than gyroscope; this could be due to higher variation of gyroscope bias relative to accelerometer. However, with the neural network approach, an improvement up to 99 % can be achieved for both accelerometer and gyroscope, which proves the superiority of the proposed method, over the traditional regression method.

For the second test in the laboratory, the IMU is manually moved with the hands in a straight line path of length 4.88 meters, which takes only 10 seconds to complete. The goal is to compare the estimated trajectory from the inertial navigation with the IMU measurements before and after compensation. As illustrated in Fig. 12, the calculated position from the raw IMU measurements drifts rapidly from its true value. The two-dimensional position error at the end of the trajectory before compensation is 21.26 m, after polynomial regression compensation, is 18.88 m, and after neural network compensation is only 0.54 m.

Finally, to further validate the effectiveness of the proposed method, a dynamic test with a car has been performed, in which a high precision IMU and a GNSS receiver from Novatel have been used as reference measurement. The trajectory from the Novatel receiver is plotted in Fig. 13 for the total duration of 30 minutes. Performing inertial navigation for the whole

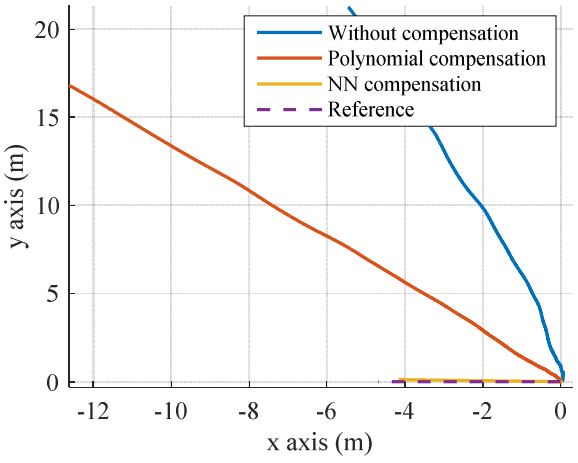

Fig. 12. Estimated trajectory from the IMU data that has been moved manually in a straight line.

duration of the test would result in a huge error in position, because of the continuous integration of acceleration and angular velocity measurements causing the accumulation of the errors over time. Therefore, instead of performing inertial navigation for the whole duration of the test, for every 60 s of the sensors output, inertial navigation is implemented for raw and compensated measurements, in order to determine the position error before and after compensation. The procedure is then repeated for the next 60 s of the measurements and so on. At the end of this procedure, position errors for 30 different portions of the measurements are obtained. Fig. 14 illustrates the average of position error over all the portions of the measurements at different elapsed times. For example, after 60 s, the average position error of the uncalibrated IMU can reach up to 4.18 km while after polynomial compensation the position error can be decreased to 2.13 km, and with the neural network compensation algorithm, the position error is less than 700 m.

VI. Conclusion

Temperature variation has a huge impact on the MEMS-based inertial sensors. Based on the observations, accelerometer bias can change from −80 mg to +110 mg in the temperature range of −25 °C to 55 °C. This indicates that a simple calibration of the deterministic errors at room temperature would not be sufficient to get acceptable results in real-world applications.

In this paper, a compensation algorithm based on the neural network is proposed, which compensates the whole measurements at once instead of modeling the error parameters (bias, scale factor, misalignment) individually. The neural network can better handle the nonlinearity inherent in sensors measurements compared to the polynomial regression.

For this purpose, a radial basis function neural network is used, and thermal compensation is considered as a function approximation problem. Both the accelerometer and gyroscope triads can be compensated by this method. To evaluate the performance of the algorithm, several tests were performed in different scenarios, including static and dynamic tests while heating the IMU. The results indicate that the neural network based approach can improve the average error up to 99 % for both accelerometer and gyroscope in a static scenario, while with the polynomial regression method with the accelerometer there is a maximum improvement of 69 %, and with the gyroscope, there is a maximum improvement of 87 %. In the dynamic test, the average position error from inertial navigation has improved by 49 % with polynomial compensation and by 81 % with the neural network compensation technique.

Numerous experiments have demonstrated that the temperature compensation method based on neural network outperforms the polynomial regression method. In order to improve the performance even more, and eliminate the remaining error after compensation, future work will address the stochastic modeling of the inertial sensor's noise and the compensation model will be tested in a GPS/INS integrated algorithm, such that GPS can provide continuous update for the INS measurements.

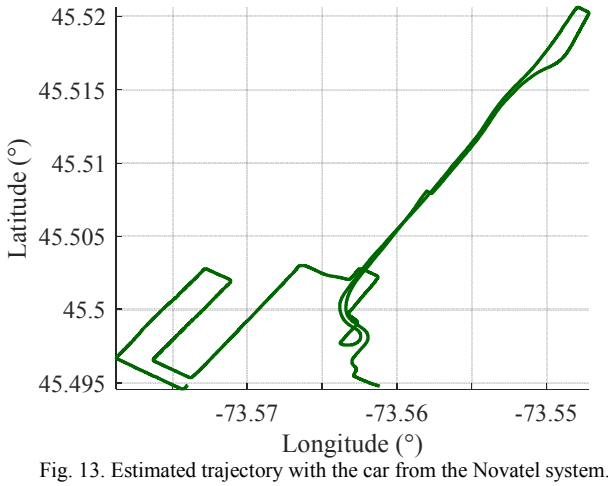

Fig. 13. Estimated trajectory with the car from the Novatel system.

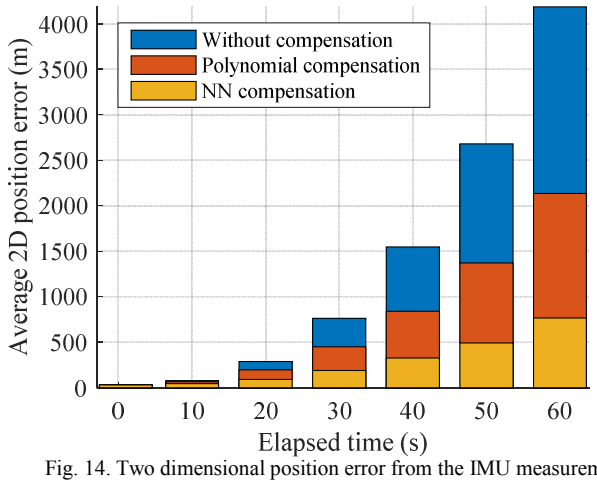

Fig. 14. Two dimensional position error from the IMU measurements.

Acknowledgment

This research is part of the project entitled VTADS: Vehicle Tracking and Accident Diagnostic System. It is supported by the Natural Sciences and Engineering Research Council of Canada (NSERC) and École de technologie supérieure (LASSENA Lab), in collaboration with two industrial partners, iMetrik Global Inc. and Future Electronics.

References

[1] M. Gad-el-Hak, *MEMS: introduction and fundamentals*: CRC press, 2005.

[2] N. Barbour and G. Schmidt, "Inertial sensor technology trends," *Sensors Journal, IEEE,* vol. 1, pp. 332-339, 2001.

[3] M. S. Grewal, A. P. Andrews, and C. G. Bartone, *Global navigation satellite systems, inertial navigation, and integration*: John Wiley & Sons, 2013.

[4] P. Aggarwal, Z. Syed, and N. El-Sheimy, *MEMS-based integrated navigation*: Artech House, 2010.

[5] D. Yang, J.-K. Woo, S. Lee, J. Mitchell, A. D. Challoner, and K. Najafi, "A Micro Oven-Control System for Inertial

Sensors," *Journal of Microelectromechanical Systems,* 2017.
[6] L. Shi Qiang, Z. Rong, and D. Heng Gao, "A temperature compensation method for micromachined thermal gas gyroscope," in *2015 IEEE Sensors, 1-4 Nov. 2015*, Piscataway, NJ, USA, 2015, pp. 1-4.
[7] C. Sheng-Ren, T. Li-Tao, C. Jen-Wei, S. Chung-Yang, L. Chih-Hsiou, C. Hong-Ren*, et al.*, "An Integrated Thermal Compensation System for MEMS Inertial Sensors," *Sensors,* vol. 14, pp. 4290-311, 03/ 2014.
[8] G. Liu, F. Yang, X. Bao, and T. Jiang, "Robust Optimization of a MEMS Accelerometer Considering Temperature Variations," *Sensors,* vol. 15, pp. 6342-6359, 2015.
[9] P. Aggarwal, Z. Syed, X. Niu, and N. El-Sheimy, "Cost-effective testing and calibration of low cost MEMS sensors for integrated positioning, navigation and mapping systems," in *Proceedings of XIII FIG Conference*, 2006, pp. 8-13.
[10] X. Niu, Y. Li, H. Zhang, Q. Wang, and Y. Ban, "Fast thermal calibration of low-grade inertial sensors and inertial measurement units," *Sensors (Switzerland),* vol. 13, pp. 12192-12217, 2013.
[11] P. Aggarwal, Z. Syed, and N. El-Sheimy, "Thermal calibration of low cost MEMS sensors for land vehicle navigation system," in *Vehicular Technology Conference, 2008. VTC Spring 2008. IEEE*, 2008, pp. 2859-2863.
[12] M. Wang, P. Guo, Z. Ren, and H. Qiu, "The new calibrating algorithm for the low-cost fiber-optics gyroscope," in *2006 IEEE/ION Position, Location, And Navigation Symposium*, 2006, pp. 739-743.
[13] R. Zhu, Y. Zhang, and Q. Bao, "A novel intelligent strategy for improving measurement precision of FOG," *IEEE Transactions on Instrumentation and Measurement,* vol. 49, pp. 1183-1188, 2000.
[14] C. Fan, Z. Jin, W. Tian, and F. Qian, "Temperature drift modelling of fibre optic gyroscopes based on a grey radial basis function neural network," *Measurement Science and Technology,* vol. 15, p. 119, 2003.
[15] R. Fontanella, D. Accardo, E. Caricati, S. Cimmino, D. De Simone, and G. Lucignano, "Improving Inertial Attitude Measurement Performance by Exploiting MEMS Gyros and Neural Thermal Calibration," in *AIAA Information Systems-AIAA Infotech@ Aerospace*, ed, 2017, p. 1134.
[16] J.-K. Shiau, C.-X. Huang, and M.-Y. Chang, "Noise Characteristics of MEMS Gyro's Null Drift and Temperature Compensation," *Journal of Applied Science and engineering,* vol. 15, pp. 239-246, 2012.
[17] Q. Zhang, Z. Tan, and L. Guo, "Compensation of temperature drift of MEMS gyroscope using BP neural network," in *Information Engineering and Computer Science, 2009. ICIECS 2009. International Conference on*, 2009, pp. 1-4.
[18] D. Xu, Z. Yang, H. Zhao, and X. Zhou, "A temperature compensation method for MEMS accelerometer based on LM_BP neural network," in *SENSORS, 2016 IEEE*, 2016, pp. 1-3.
[19] X. Chen and C. Shen, "Study on temperature error processing technique for fiber optic gyroscope," *Optik-International Journal for Light and Electron Optics,* vol. 124, pp. 784-792, 2013.
[20] L. Wang, Y. Hao, Z. Wei, and F. Wang, "Thermal calibration of MEMS inertial sensors for an FPGA-based navigation system," in *3rd International Conference on Intelligent Networks and Intelligent Systems, ICINIS 2010, November 1, 2010 - November 3, 2010*, Shenyang, China, 2010, pp. 139-143.
[21] Y. Feng, X. Li, and X. Zhang, "An Adaptive Compensation Algorithm for Temperature Drift of Micro-Electro-Mechanical Systems Gyroscopes Using a Strong Tracking Kalman Filter," *Sensors,* vol. 15, pp. 11222-11238, 2015.
[22] Y.-s. Zhang, Y. Wang, T. Yang, R. Yin, and J. Fang, "Dynamic angular velocity modeling and error compensation of one-fiber fiber optic gyroscope (OFFOG) in the whole temperature range," *Measurement Science and Technology,* vol. 23, p. 025101, 2012.
[23] Y. Zhang, Y. Guo, C. Li, Y. Wang, and Z. Wang, "A New Open-Loop Fiber Optic Gyro Error Compensation Method Based on Angular Velocity Error Modeling," *Sensors,* vol. 15, pp. 4899-4912, 2015.
[24] M. El-Diasty and S. Pagiatakis, "Calibration and stochastic modelling of inertial navigation sensor errors," *Journal of Global Positioning Systems,* vol. 7, pp. 170-182, 2008.
[25] D. Titterton and J. L. Weston, *Strapdown inertial navigation technology* vol. 17: IET, 2004.
[26] M. J. Orr, "Introduction to radial basis function networks," ed: Technical Report, Center for Cognitive Science, University of Edinburgh, 1996.
[27] S. S. Haykin, *Neural networks and learning machines* vol. 3: Pearson Upper Saddle River, NJ, USA:, 2009.
[28] Z. Zainuddin and O. Pauline, "Function approximation using artificial neural networks," *WSEAS Transactions on Mathematics,* vol. 7, pp. 333-338, 2008.